

# MESOSCALE EDDIES IN THE NORTHWESTERN PACIFIC OCEAN: THREE-DIMENSIONAL EDDY STRUCTURES AND HEAT/SALT TRANSPORTS

Di Dong

South China Sea Institute of Planning and Environmental Research, SOA, Guangzhou, China, dongdide90@126.com

## ABSTRACT

The region encompassing the Kuroshio Extension (KE) in the Northwestern Pacific Ocean (25N–45N and 130E–180E) is one of the most eddy-energetic regions of the global ocean. The three-dimensional structures and transports of mesoscale eddies in this region are comprehensively investigated by combined use of satellite data and Argo profiles. With the allocation of Argo profiles inside detected eddies, the spatial variations of structures of eddy temperature and salinity anomalies are analyzed. The results show that eddies predominantly have subsurface (near-surface) intensified temperature and salinity anomalies south (north) of the KE jet, which is related to different background stratifications between these regions. A new method based on eddy trajectories and the inferred three-dimensional eddy structures is proposed to estimate heat and salt transports by eddy movements in a Lagrangian framework. Spatial distributions of eddy transports are presented over the vicinity of the KE for the first time. The magnitude of eddy-induced meridional heat (freshwater volume) transport is on the order of 0.01 PW ( $10^3 \text{ m}^3/\text{s}$ ). The eddy heat transport divergence results in an oceanic heat loss south and heat gain north of the KE, thereby reinforcing and counteracting the oceanic heat loss from air-sea fluxes south and north of the KE jet, respectively. It also suggests a poleward heat transport across the KE jet due to eddy propagation.

## INTRODUCTION

As an energetic eastward flowing inertial jet, the Kuroshio Extension (KE) is characterized and surrounded by a complicated ocean circulation structure (Fig. 1). The KE sheds off vigorous mesoscale eddies toward north and south, which in turn interact with the fronts. Mesoscale eddies contribute to the meridional heat and salt transport in the North Pacific, impacting the Kuroshio path, regional hydrography, water mass modification, marine biology, fisheries, and even the overlaying atmospheric boundary wind, rain and storm tracks. Mesoscale eddies have been extensively investigated by hydrographic measurements from research vessels and autonomous platforms like Argo floats and gliders, infrared imagery, altimetry data as well as model simulations in the past 40 years. But few have examined spatial variations of eddy structures and eddy-induced heat and salt transport there. The existing remote sensing data set of SLA, together with Argo float profiles makes it possible for us to further investigate the potential influences of Kuroshio eddies on the three-dimensional temperature and salinity fields of the upper ocean, and to estimate the eddy-induced meridional and zonal transports of heat and salt in the Northwestern Pacific Ocean, encompassing the KE region.

## OBJECTIVES

The objectives of this paper are (1) to calculate and analyze spatial variations of eddy structures in the Northwestern Pacific Ocean (from 25N to 45N, from the Japanese coast to 180E) and (2) to investigate eddy heat and salt transports within a Lagrangian framework.

## DATA AND METHODS

Mesoscale eddies were detected with the delayed-time reference data “two-sat-merged” SLA (version 2014), produced and distributed by the CMEMS (Copernicus Marine and Environment Monitoring Service) over the period from January 2000 to December 2014. The vertical structures of mesoscale eddies were investigated with Conductivity-Temperature-Depth (CTD) profiles from Argo floats taken in the study region from January 2000 to December 2014 provided by the Coriolis Global Data Acquisition Center of France. To reveal the intensive air-sea interactions in the KE, the mean atmospheric net heat flux was derived from the long-term monthly means of the National Centers for Environmental Prediction-National Center for Atmospheric Research (NCEP-NCAR) reanalysis data during years 1981–2010, with a spatial resolution of  $2.5^\circ$ . To calculate the heat and salt transports by eddy movements, we use the “Mesoscale Eddy Trajectory Atlas” Product and the third version of eddy trajectories based on weekly SLA data from Chelton et al. (2011; CH12) for comparison.

The eddy detection method of Faghmous et al. (2015; FAG) is used to obtain eddy boundaries. By collocating Argo float profiles and detected eddies in time and space, the eddy-induced property anomalies are obtained by subtracting from the considered profile a local mean climatological profile computed by averaging all available profiles acquired outside eddies and within a spatial (temporal) radius of 200 km (30 days) from the position (date) of the considered profile. To calculate three-dimensional eddy structures, all anomalies are transformed onto an eddy-coordinate space and mapped onto  $10 \text{ km} \times 10 \text{ km}$  grids with the inversed distance weighting (IDW) interpolation. For each grid point, profiles with a radius of influence  $R=60 \text{ km}$  are assigned with a weight value for interpolation. To study the meridional and zonal variations of eddy structures, we divide the study region into nine subregions ( $10^\circ \times 10^\circ$  boxes) (Fig. 2). Eddy trajectory atlas is combined with the obtained three-dimensional eddy structures to formulate a new method to estimate eddy heat and salt transports. The divergence of the heat transport is compared with the mean atmospheric net heat flux and two-dimensional Loess filter with half width of  $10^\circ$  longitude and  $5^\circ$  latitude.

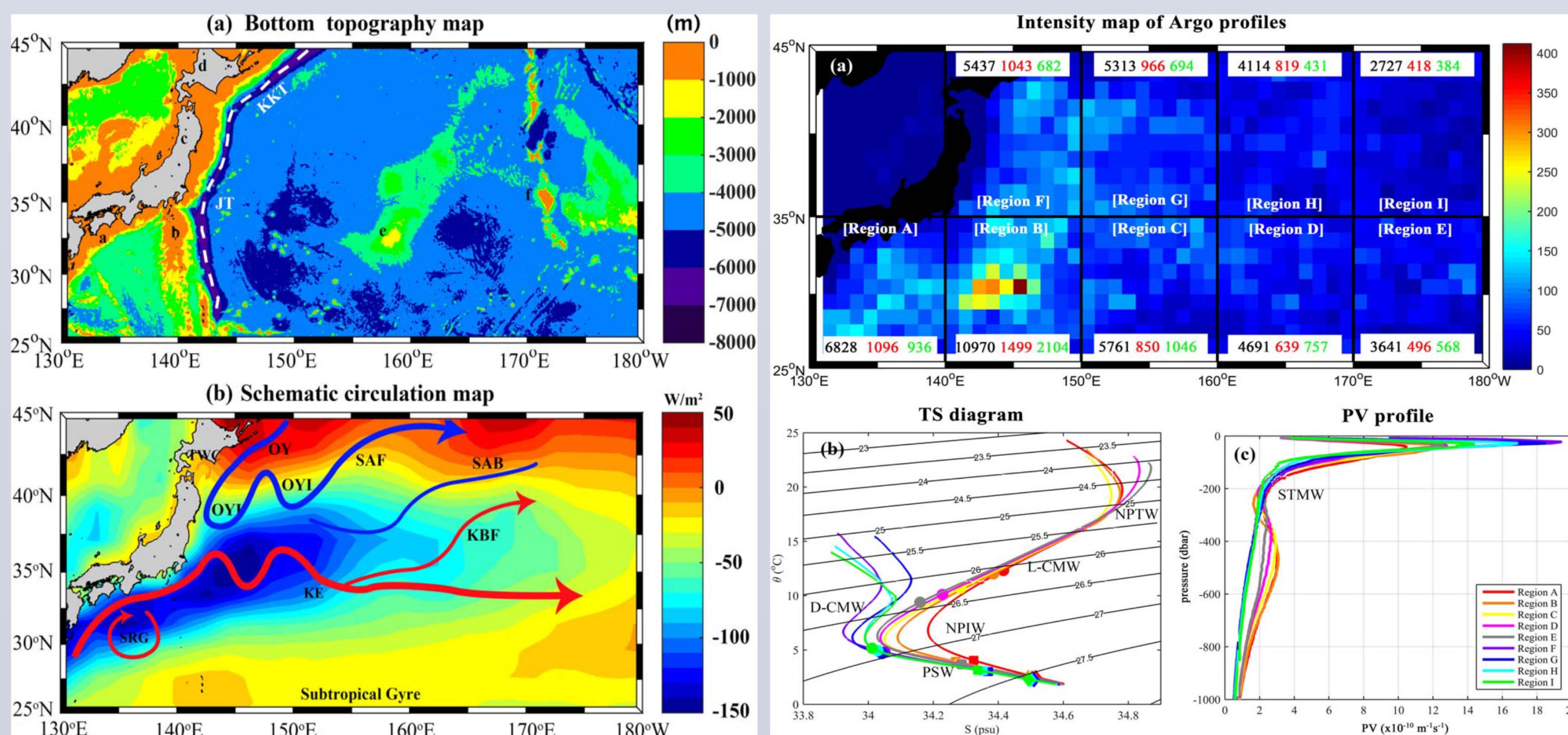


Fig. 1. Bottom topography map (a) and schematic circulation map (b) in the Northwestern Pacific Ocean. The color in (b) is annual mean net surface heat flux from the NCEP-NCAR reanalysis data. Fig. 2. (a) Intensity map of Argo profiles in the period 2000–2014. Red: AE, green: CE, black: outside of eddies. TS diagrams (b) and PV profiles (c) of all subregions.

## RESULTS

Fig. 3 show the mean temperature anomaly profiles for eddies in the nine subregions north and south of the KE. The eddy-induced temperature anomaly reach  $1\text{--}2^\circ\text{C}$  in the main thermocline, and a large discrepancy exists in the meridional direction. Eddy structures are dominated by subsurface anomalies south of the KE; while north of the KE, eddy-induced anomalies are intensified near the surface.

The gradual change in the eddy-induced temperature anomaly structure with longitude north and south of the KE is shown in Fig. 4. For AEs south of the KE (135E–180E), the westward strengthening and deepening of eddy signals is evident. North of the KE, AEs in region F show cold and fresh signals in the depth range 400–800 dbar, making the westward strengthening eddy signal (in terms of anomaly magnitude) only evident in the upper water layers.

The vertical sections of the mean temperature anomaly of the composite AEs and CEs at different pressure levels are shown in Fig. 5. Most eddy cores are shifted to the west with large anomalies in the west of or near the KE jet (except region A), suggesting poleward heat transports by mesoscale eddies. The anomaly magnitude decreases with depth, having little impact below 1,000 dbar.

The meridional eddy heat transports calculated from our method and modified method by Zhang et al. (2014; MZ method) in the KE region are compared in Fig. 6. The trends and values of the total meridional eddy heat transports are consistent for both methods. The total meridional eddy heat transport values are smaller in magnitude in regions 25N–30N and 40N–45N than the region near the KE jet, suggesting that eddies shed off the KE are the main contributors to the poleward eddy heat transport. The magnitude of eddy-induced meridional heat transport is on the order of 0.01 PW. Fig. 7 shows the distribution of meridional eddy heat transport in the Northwestern Pacific Ocean from our method based on CH17 data.

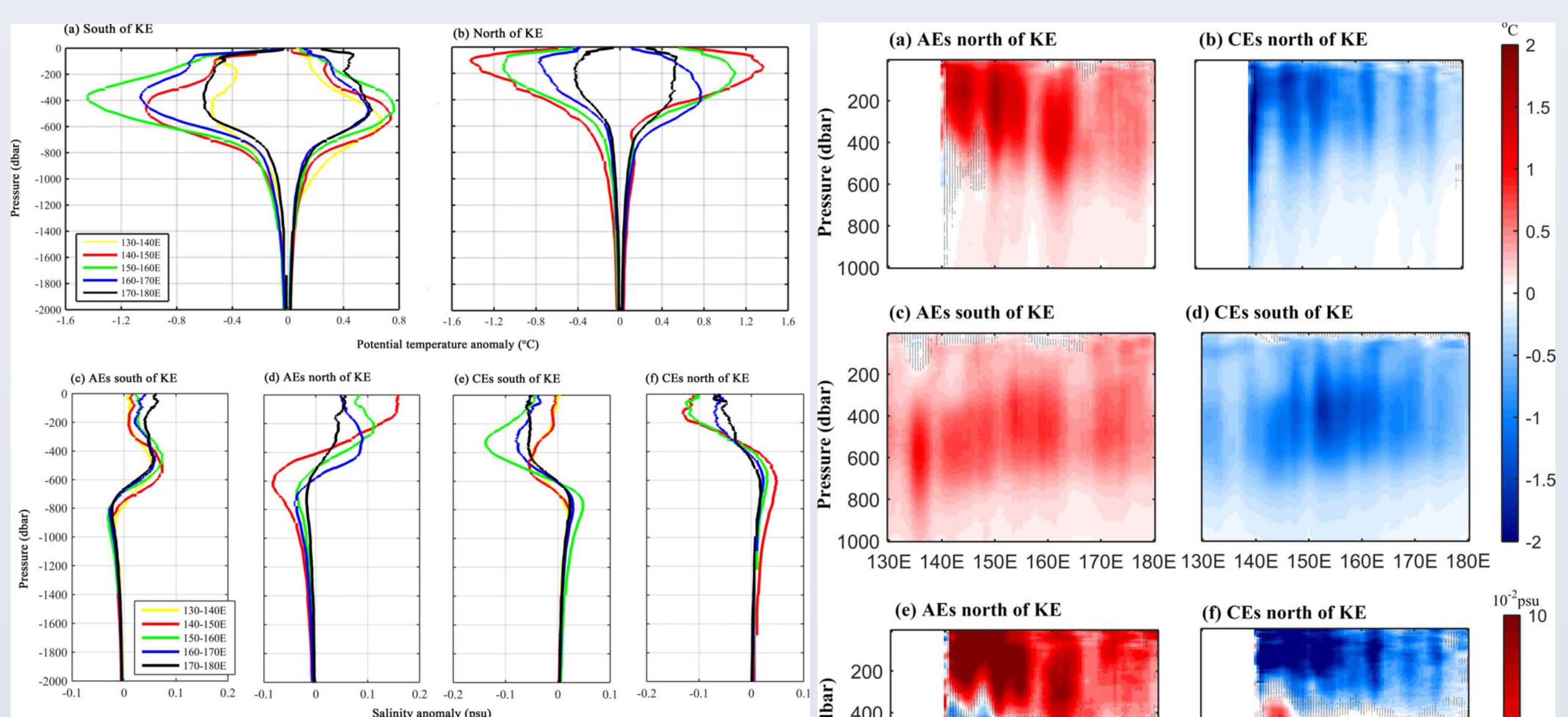


Fig. 3. Mean profiles of temp. anomalies for AE and CE in all subregions (a) south and (b) north of the KE.

Fig. 4. Temp. anomaly of (a, c) AEs and (b, d) CEs as function of longitude (a, b) north and (c, d) south of the KE. Salinity anomaly of (e, g) AEs and (f, h) CEs as function of longitude (e, f) north and (g, h) south of KE.

Fig. 5. The 3-D structures of temp. anomaly for (a) AEs in region H and (b) CEs in region C.

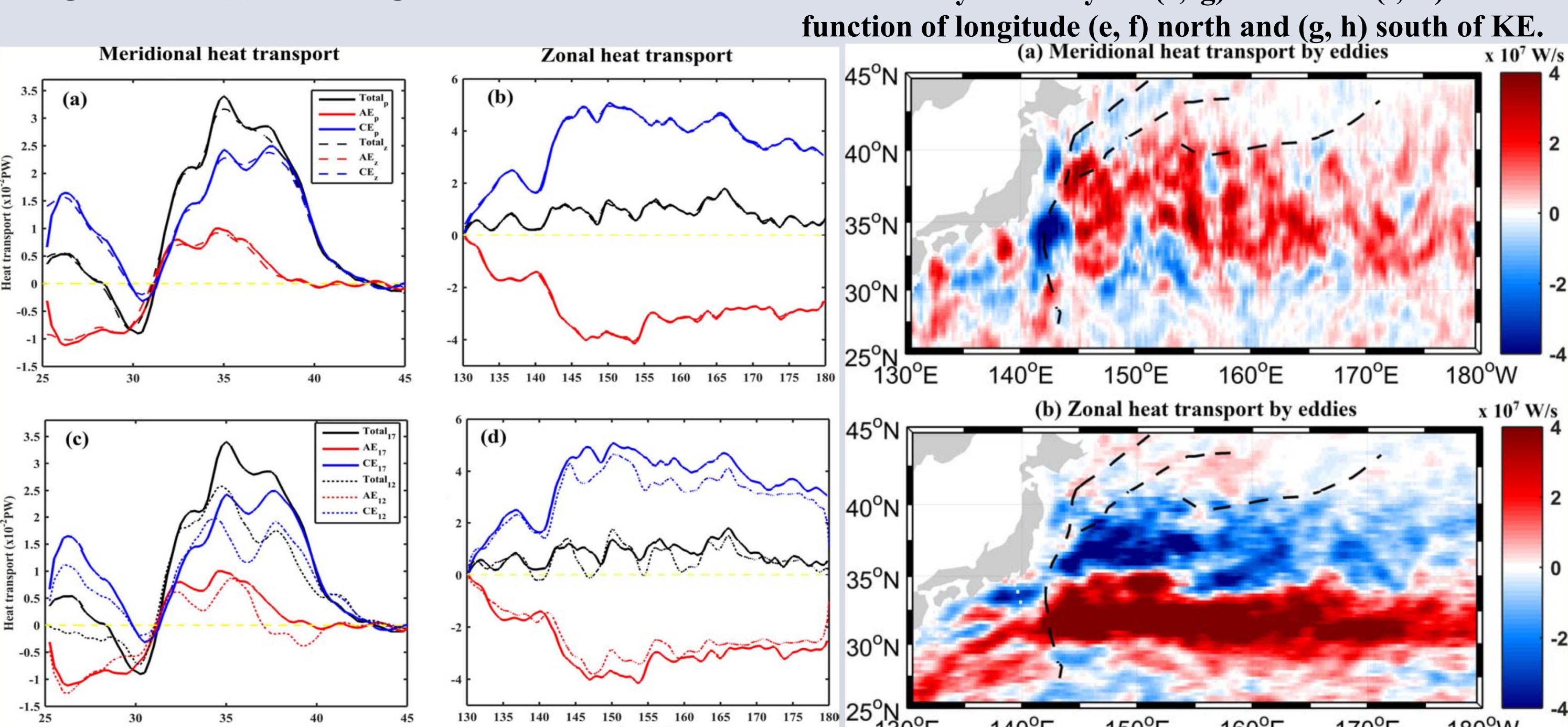


Fig. 6. The (a) meridional and (b) zonal heat transport by eddies from our method (based on the meridionally integrated zonal heat transport by CH17 data). Fig. 7. (a) Meridional heat transport by eddies, (b) zonal heat transport by eddies. Fig. 8. (a) Meridional heat transport by eddies, (b) zonal heat transport by eddies.

## SUMMARY

Zonal and meridional variations of three-dimensional eddy structures are investigated in the Northwestern Pacific Ocean. A new method is proposed to estimate the spatial distributions of eddy heat and salt transports in a Lagrangian framework. Negative/positive divergence of eddy heat transport north/south of the KE suggests a poleward eddy heat transport across the KE jet.

## REFERENCES

Dong, D., Brandt, P., et al. (2017). Mesoscale eddies in the Northwestern Pacific Ocean: Three-dimensional eddy structures and heat/salt transports. *Journal of Geophysical Research: Oceans*, 122.